Chapter 33
Multisensor Global Retrievals of Evapotranspiration for Climate Studies Using the Surface Energy Budget System

Matthew McCabe, Eric Wood, Hongbo Su, Raghuveer Vinukollu, Craig Ferguson, and Z. Su

33.1 Introduction

Evaporation from water or soil surfaces and transpiration from plants combine to return available water at the surface layer back to the bulk atmosphere in a process called evapotranspiration. Much of our understanding of the complex feedback mechanisms between the Earth's surface and the surrounding atmosphere is focused on quantifying this process. At its most fundamental level, evapotranspiration is the loss of water from a surface to the atmosphere, achieved through vaporization. The complex nature of the evaporative process, however, includes mechanisms such as turbulent transport, feedback between the surface and atmosphere, and the biophysical nature of transpiration – all of which combine to make both measurement and estimation a difficult task.

Evapotranspiration is one of the most important components of the hydrological cycle, and together with precipitation, also represents the most spatially variable. Combined with rainfall and runoff, it controls the availability and distribution of water at the Earth's surface, and therefore, is significant to a number of research fields. An increased understanding of surface energy interactions broadly contributes to agricultural, hydrological, and climatological investigations. For instance, accurate routine estimation of evapotranspiration provides the following advantages: (a) improve water management practice by estimating recharge in groundwater aquifers or evaporative loss from open water bodies; (b) improve irrigation and water use management for agricultural purposes, particularly in water-intensive farming practice; (c) provide needed constraints in plant growth, carbon and nutrient cycling and production modeling; (d) inform catchment modeling applications; and (e) improve understanding of larger-scale meteorological and climatological applications.

M. McCabe (✉)
Department of Civil and Environmental Engineering,
University of New South Wales,
Sydney, NSW 2052, Australia
e-mail: mmccabe@unsw.edu.au

B. Ramachandran et al. (eds.), *Land Remote Sensing and Global Environmental Change*, Remote Sensing and Digital Image Processing 11, DOI 10.1007/978-1-4419-6749-7_33,

While evaporation itself is a conceptually simple process, it has proved extremely difficult to accurately describe or characterize for natural surfaces and systems. Apart from difficulties representing aspects of the physical mechanisms mentioned above, heterogeneities at the land surface, and to a lesser extent in the atmosphere (Raupach and Finnigan 1995), the interacting influences and feedbacks in the soil, vegetation and meteorological continuum (Trenberth 1999) and imprecise knowledge of component variables, all contribute to complicate a relatively fundamental theoretical basis. Much effort was directed, over the course of the last three decades, toward developing techniques to quantify evapotranspiration at the land surface using remotely sensed data, in recognition of the critical role they play in many environmental processes. The multitude of techniques subsequently developed to measure or model evapotranspiration vary considerably in the extent of their complexity (see Kalma et al. 2008 for a review).

The variability of evapotranspiration in space and time is influenced by changes in atmospheric condition, land use, vegetation, soils, and topography. Additionally, even where high quality local-scale data may exist, land surface heterogeneity complicates the extrapolation of point source surface flux estimates to larger scales (McCabe and Wood 2006; Li et al. 2008; Brunsell et al. 2008). Currently, it is possible only to accurately measure the latent and sensible heat from the land surface at relatively small spatial scales.

Although evapotranspiration is quantifiable at the small scale using ground-based techniques, larger-scale estimates require alternative measurements and estimation approaches. A lack of such measurements and knowledge hinders the closure of the land surface energy and water balances for regional and larger spatial scales, and impedes the development of suitable land surface parameterizations schemes. Implementing a routine methodology that circumvents the limitations imposed by spatial and temporal heterogeneity necessitates the use of a remote sensing approach to adequately account for such variability. Determining the level of spatial and temporal resolution appropriate for the modeling task is a difficult process, especially because of the lack of a consistent theory to move between scales (Beven and Fisher 1996).

Traditionally, evapotranspiration estimation is limited by the availability of spatially distributed datasets, with analyses subsequently focusing on the field or catchment scale of observation. Remote sensing of the land surface offers a number of unique advantages over conventional field-based data collection. Foremost among these is the spatial extent of data, facilitating observations from local to continental scales. Also, the potential to examine areas at multiple scales due to the array of sensors available, which offer a variety of spatial, spectral, and temporal characteristics exists. There also exist a number of limitations: in particular, the compromise between resolving an appropriate spatial scale and an adequate temporal frequency.

Applications are the primary drivers, which determine the appropriateness of the spatial and temporal scale. For instance, high spatial resolution (sub-100 m)/low temporal frequency (multiweekly) satellites such as Landsat and ASTER offer excellent opportunities to resolve field-scale evapotranspiration for use in agricultural and irrigation applications (Gowda et al. 2007; Glenn et al. 2007), with a number of approaches being used precisely for this purpose (Bastiaanssen et al. 1998; Allen et al. 2007). In contrast, geostationary satellite platforms (GOES, MeteoSat, FY-2, MTSat) compromise lower spatial resolution (>1 km) with increased temporal frequency (sub-hourly) to provide unparalleled coverage. Recent advances in remote estimation of evapotranspiration with geostationary platforms show considerable promise to provide needed surface retrievals (Norman et al. 2003; Anderson et al. 2007), and partially address the issue of cloud cover influences on infrared surface temperature retrieval through increased temporal frequency.

For climate studies, global coverage using consistent methods and sensors remains a long-term goal of the NASA Energy and Water Cycle Study (NEWS). The Moderate resolution Imaging Spectroradiometer (MODIS) sensor on board the Aqua and Terra satellites, together with other satellites within NASA's Earth Observing System (EOS), offers an excellent compromise between the competing spatial and temporal requirements described above. MODIS contributes moderate resolution (1 km) data at multiple times throughout the diurnal cycle, and therefore remains an extraordinarily valuable resource in the Earth observation.

The focus of the present contribution is a discussion on the application of MODIS and other NASA Earth Observing satellites toward providing consistent global evapotranspiration retrievals. Through a systematic retrieval approach that develops evapotranspiration estimates across local, regional, and continental scales, we illustrate the potential of such products to provide insight and characterization of the land surface for a variety of essential applications.

33.2 Modeling Evapotranspiration

The need to effectively measure regional-, as opposed to point-scale estimates of evapotranspiration, has witnessed the development of a number of modeling approaches. However, the complications mentioned above render the characterization and physical description of evapotranspiration difficult. Of particular interest is the effective representation of the near-surface interaction with the lower atmosphere, especially in the context of generalized circulation models (GCMs). This interest is rendered challenging by land surface schemes, which are commonly inadequate for modelers, who examine such issues as climate prediction or climate change scenarios. A balance between increased model complexity and parsimony of model structure is required, particularly in the light of parameter uncertainty and model validation limitations.

33.2.1 Surface Energy Balance System: The Interpretive Model

It is widely accepted that remote sensing has the potential to spatially characterize the evapotranspiration, but it is ineffective on its own, in characterizing the range of processes operating on the land surface. To effectively use satellite-derived remote sensing data to produce reliable estimates of evapotranspiration, the derived products require incorporation into an interpretive modeling framework.

The approach employed here is based on Su's (2002) Surface Energy Balance System (SEBS) model. SEBS was developed to estimate surface heat fluxes using satellite earth observation data in combination with routinely available meteorological forcing. SEBS is one of a family of similarly constructed models that consider the land surface via electrical analogue; that is, they regard the exchange of heat flux between the surface and atmosphere as driven by a difference in temperature (a potential) with the rate controlled by a number of resistances that depend on local atmospheric conditions, and land surface and vegetation characteristics.

SEBS falls into a general class of micro-meteorological evapotranspiration models that require a near surface and 2-m air temperature gradient, net radiation and other surface meteorology to drive model estimates. A variety of sophisticated approaches are available to estimate evapotranspiration in this manner. For excellent reviews and additional information, refer Kustas and Norman (1996), Quattrochi and Luvall (1999), Kalma et al. (2008) and Verstraeten et al. (2008). Further details on the SEBS model are available in the works of Su (2002), Su et al. (2005) and McCabe and Wood (2006).

33.2.2 Data Sources

Although remote sensing methods cannot measure the evaporative process directly, they do offer a means to extend point measurements to larger scales and also provide information on specific components and variables needed for energy and moisture balance estimation. Coupling remotely sensed information with ground-based data allows much greater insight into the dynamics of larger-scale processes than available from either source alone. The following section details data sources required by SEBS, obtainable from either remote sensing directly or through operational products. Many of the variables required by SEBS are discussed in greater detail elsewhere in this book, so only those data, which require significant modifications are presented.

33.2.2.1 Remote Sensing Variables

1. *Land surface temperature and emissivity*: Land surface temperature estimates are integral in the quantification of energy fluxes, and help estimate evapotranspiration. The MOD11 Surface Temperature product provides the key variable to determine surface fluxes from space. Remotely sensed land surface temperatures are used in a number of applications including monitoring of the surface radiation budget (Nunez and Kalma 1996), modeling of regional scale evapotranspiration (McCabe and Wood 2006), land surface flux estimation (Kustas and Norman 1996; Su et al. 2005), and also assist in moisture availability studies (McVicar and Jupp 2002). SEBS directly uses LST estimates to calculate net

radiation. To determine this value, a broadband emissivity is also needed, which is derived from the daily MODIS (bands 29, 31, and 32) narrow band emissivity estimates (Wan et al. 2002).

2. *Shortwave radiation*: Measuring the individual components which constitute net radiation from space is a difficult task. Due to instrument configuration, many satellites used to derive shortwave radiative fluxes to accurately detect important influences on the radiation budget such as snow cover, cloud and/or aerosol optical properties. The MODIS instrument allows insight into global monitoring of atmospheric profiles, column water vapor amount, aerosol particles, and cloud properties with higher accuracy and consistency than previous Earth observation imagers (King et al. 1992). These simultaneous observations are enormously useful to accurately derive surface radiative fluxes.

   Recent experiments using MODIS swath-based shortwave radiation data to estimate flux (Su et al. 2008) indicate much promise. To enable the use of independently derived optical parameters from multispectral satellites such as MODIS, the GEWEX-Surface Radiation Budget (SRB) model (Pinker and Laszlo 1992; Pinker et al. 2003), was modified to use with such observations, and tested with MODIS-based parameterizations. Parameters required to drive the SRB model include the following: viewing geometry, column water vapor, column ozone amount, cloud fraction, cloud optical thickness, aerosol optical depth, and spectral surface albedo – all of which are available from either Terra/Aqua MODIS or the NASA A-Train satellite series. The feasibility to implement this approach with MODIS data at various spatial scales is described in Pinker et al. (2003). Preliminary results on inferring radiative fluxes from MODIS information show that the modified version of GEWEX/SRB is able to use MODIS-derived optical and ancillary information (Su et al. 2008). In previous applications (e.g., Su et al. 2005), the Geostationary Operational Environmental Satellite (GOES) data were used to determine net shortwave. Merging the temporal information available from GOES with the spatial resolution of MODIS data provides a very valuable radiation resource.

3. *Albedo*: Chapter 24 presents a detailed description of the MOD43 Broadband Albedo product (Schaaf et al. 2002). Although a true surface albedo product is not currently available, an average of the black-sky and white-sky albedo available from MOD43 was previously used. Assuming an even distribution between direct (black-sky) and diffuse (white sky) radiation are not likely true under all surface and atmospheric conditions, studies suggest this will provide a reasonable approximation (Wang et al. 2004). To address this shortcoming, a more representative surface albedo requires consideration of atmospheric optical depth and water vapor. Current SEBS applications, which use MOD09 spectral reflectance data, and follow Liang et al. (1999), are expected to provide a more accurate characterization of this variable.

4. *Vegetation indices*: Vegetation indices such as the Normalized Difference Vegetation Index (NDVI), available as part of the MODIS Vegetation Index Product (MOD13) (Chap. 26), and the MODIS Leaf Area Index (LAI) and Fraction of Photosynthetically Active Radiation (fPAR) Product (MOD15)

(Chap. 27), form integral components of the SEBS model. Specifically, LAI and vegetation fraction, which are derived from the NDVI, are used to estimate: (a) the roughness height for heat and momentum transfer; (b) the mixed emissivity when remote sensing data are employed (to derive the surface temperature); and (c) the ground heat flux over a region, if unavailable from measurements.

A number of authors have previously related measured vegetation indices to ground-based records of LAI (Su 2000). Correctly representing the variation of the vegetation is crucial to obtain accurate reproduction of the surface fluxes. Further details of these variables are available in the Chapters listed above.

33.2.2.2 Meteorological Forcing

Coupling remotely sensed information with ground-based data allows much greater insight into the dynamics of larger-scale processes than is available from either source alone. Traditionally, there is a disconnect between the spatially dense nature of remote sensing observation and the sparse distribution of meteorological networks. The North American Land Data Assimilation System (NLDAS) (Mitchell et al. 2004) addresses the lack of spatially and temporally consistent data by gathering best quality, modeled and observed, meteorological fields to produce both real time (1999) and retrospective forcing. NLDAS forcing data are primarily derived from the National Centers for Environmental Prediction (NCEP) Eta Model-based Data Assimilation (EDAS) (Rogers et al. 1996) output.

Meteorological forcing data, such as wind velocity, humidity, pressure, air temperature, and downward longwave radiation, are extracted from the NLDAS to allow SEBS-based estimation of evapotranspiration. NLDAS has a spatial resolution of 0.125°, and provides information at an hourly time step. It is extensively validated and implemented as a dataset for land surface modeling (Luo et al. 2003). The reliance on spatial fields of forcing data clearly restricts broader scale application of SEBS in areas where such data are not available. The recent development of both a Global Land Data Assimilation (GLDAS) (Rodell et al. 2004) and the Land Information System (LIS) (Kumar et al. 2006) offers the possibility to routinely estimate SEBS-derived surface fluxes in data-sparse areas. Additionally, advances in retrieving solar radiation from MODIS (Pinker et al. 2003), and the ability to retrieve atmospheric variables, such as air temperature, from the MODIS Atmospheric profile product (MOD07) (e.g., Bisht et al. 2005) will improve the capacity to globally estimate evapotranspiration by removing the reliance on surface-based meteorological observations.

33.3 Algorithm Validation

SEBS requires evaluation against diverse data to assess its potential to routinely estimate global-scale evapotranspiration. Specifically, the SEBS model requires evaluation across a variety of climate zones and land covers, thereby assessing the adaptability of the model to climate and land cover variability. To fulfill this goal, a validation dataset satisfying these criteria is required. Here we present two published case studies at different spatial extents that illustrate the progressive nature of validation efforts with SEBS. Good quality surface tower-derived flux data, together with meteorological forcing from both in-situ measurement and operational meteorological datasets are used to assess the model's ability to reproduce flux retrievals.

Further details on the results presented here are available in Su et al. (2005).

33.3.1 Local- and Regional-Scale Flux Validation

An assessment of SEBS' ability to reproduce observed fluxes was performed using independent high-quality data collected during the Soil Moisture Atmospheric Coupling Experiment (SMACEX 02) (Kustas et al. 2005), a crop land-based field campaign in the Walnut Creek catchment in southern Iowa (see Figure 1 of McCabe and Wood 2006). The objectives of this investigation include the following: (1) evaluate SEBS estimates using local-scale (tower) data to determine the accuracy limit at the field scale; and (2) identify the potential to use operational meteorology from the NLDAS coupled with high-resolution Landsat data to predict spatially distributed surface fluxes. Flux measurements from ten eddy covariance systems positioned on towers throughout the catchment were used to evaluate SEBS across both corn and soybean fields.

Independent measurements of the latent and sensible heat fluxes were derived using a 3-D sonic anemometer and a LiCor 7500 water vapor/CO_2 sensor (Kustas et al. 2004). These independent measurements permit a user to make an energy balance closure assessment since the net radiation and soil heat flux are also observed. To address the non-closure problem, a characteristic of much eddy-covariance flux data, a Bowen ratio closure method was employed to correct the sensible and latent heat flux measurements (Twine et al. 2000). Further information on the correction of the eddy covariance data with such closure techniques is provided in the study of Prueger et al. (2005a, b).

33.3.1.1 Results from Local-Scale (Tower Based) Forcing Data

The in-situ measurements required by SEBS are listed in Table 33.1. In addition to tower-based flux measurements, detailed vegetation parameters and hydrometeorological data were collected during the SMACEX 02 campaign (Kustas et al. 2005). In this analysis, in-situ observations of incoming solar radiation (insolation), downward longwave radiation and soil heat flux were used directly in SEBS to compute the available energy. Meteorological and heat flux data were resampled to 30-min intervals. Standard meteorological forcing data including wind velocity, vapor pressure, air temperature, and atmospheric pressure were used to run the SEBS model.

Table 33.1 SEBS model data requirements

Data type	Variables	Unit
Surface meteorological data	Air temperature	°C
	Pressure	kPa
	Wind	m/s
	Vapor pressure	kPa
Radiative energy flux	Incident shortwave radiation	W/m^2
	Outgoing shortwave radiation	W/m^2
	Incident longwave radiation	W/m^2
	Outgoing longwave radiation	W/m^2
	Net radiation	W/m^2
Surface heat flux	Ground heat flux	W/m^2
	Sensible heat flux	W/m^2
	Latent heat flux	W/m^2
	Evaporative fraction	–
Surface temperature	Composite radiometric temperature (soil + vegetation)	°C
Vegetation parameters	Vegetation height	M
	Vegetation fraction	–
	Leaf area index	–
	Vegetation type (corn or soybean)	–

Land surface temperature, a key variable in the SEBS model application, was measured by Apogee infrared thermometers (model IRTS-P) (Jackson and Cosh 2003a). LAI and vegetation fraction were used to estimate the following: (a) the roughness height for heat and momentum transfer; (b) the mixed emissivity when remote sensing data are employed (to derive the surface temperature); and (c) the ground heat flux over a region, if unavailable from measurements. LAI, vegetation fraction and vegetation height were measured on four separate occasions (June 18th, 28th, and July 2nd, 5th). A simple linear interpolation was used to generate daily LAI and vegetation height throughout the study period from the observations. Studies have observed that the relationship between the vegetation fraction and LAI is often nonlinear (Chen and Cihlar 1995), which potentially cause inconsistency between vegetation parameters if a linear interpolation is used. Thus, a nonlinear relationship between LAI and vegetation fraction was formulated to make full use of the vegetation measurements, and maintain consistency between observations (see Su et al. 2005 for further details).

SEBS was run at a temporal resolution of 30 min from 10:00 to 16:00 local solar time, at each of ten flux tower sites for the 20-day duration of SMACEX 02. The SEBS model-estimated evapotranspiration was compared with eddy covariance-based flux observations, which allowed an assessment of the model's accuracy. Figure 33.1 shows the SEBS-derived evapotranspiration scatter plots against the SMACEX-observed latent heat flux. For five corn sites (Fig. 33.1a), an even distribution about the 1:1 line and an r^2 of 0.89 illustrates the consistent agreement between estimates and measured fluxes. A root mean squared error (RMSE) of 46.68 W m^{-2} and a mean absolute error (MAE) of 36.14 W m^{-2} indicate a performance comparable to an in-situ flux observation technique's error.

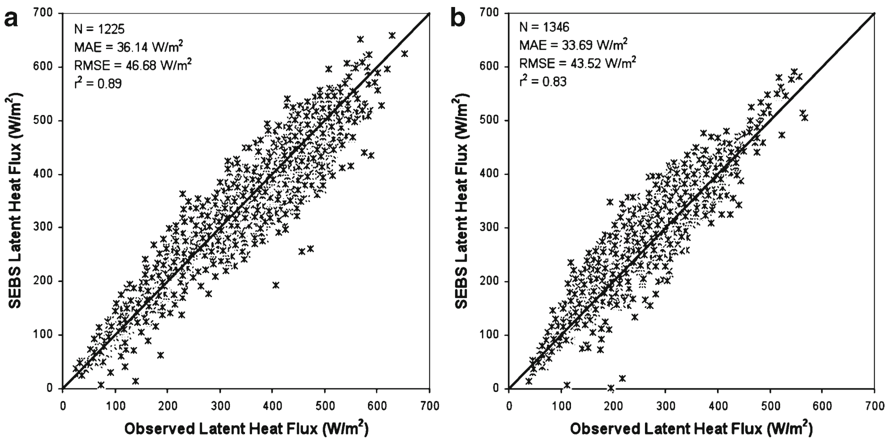

Fig. 33.1 SEBS tower-based predictions of latent heat flux versus eddy covariance observations for (**a**) corn and (**b**) soybean field sites. Associated statistics from analysis are included in the plots

During the first 10 days of SMACEX, results indicated that SEBS overestimated the latent heat flux for two of the five soybean sites. Although a number of possible explanations for the inconsistent performance at these locations exist (homogeneity in downward longwave forcing data; variations in energy balance closure; variations in vegetation information or surface temperature), closer examination of the two biased sites indicated that the vegetation fractions were the lowest for all observation locations. A decreased vegetation fraction results in an overestimation of the emissivity. To address this, a new effective emissivity was calculated at these locations by assigning a vegetation emissivity of 0.98 and a soil emissivity of 0.94 (following Chen et al. 2004). Model outputs for the emissivity-corrected sites present improved agreement with an RMSE of 43.52 W m^{-2}, an MAE of 33.69 W m^{-2} and an r^2 of 0.83 (see Fig. 33.2b).

Results of this point scale analysis indicate SEBS can accurately reproduce surface fluxes over varied vegetation and hydrometeorological conditions.

33.3.1.2 Results from the Regional-Scale (NLDAS) Forcing Data

In-situ measurements are not generally available for model forcing to routinely estimate surface fluxes. As a result, data from satellite and operational meteorology offer the best surrogate for local measurements. Table 33.2 shows the outline of the data requirements and sources of the meteorological and satellite products employed in the regional-scale analysis. The data represent a variety of resolutions and interpolation is used where necessary to standardize the measurements. To complement the availability of Landsat-ETM surface temperature data (Li et al. 2004), NLDAS forcing data at 11 AM were used in place of the tower-based meteorology, offering an opportunity at examine a more operationally based estimate of surface fluxes. In addition, high-resolution (30 m) land cover classification and

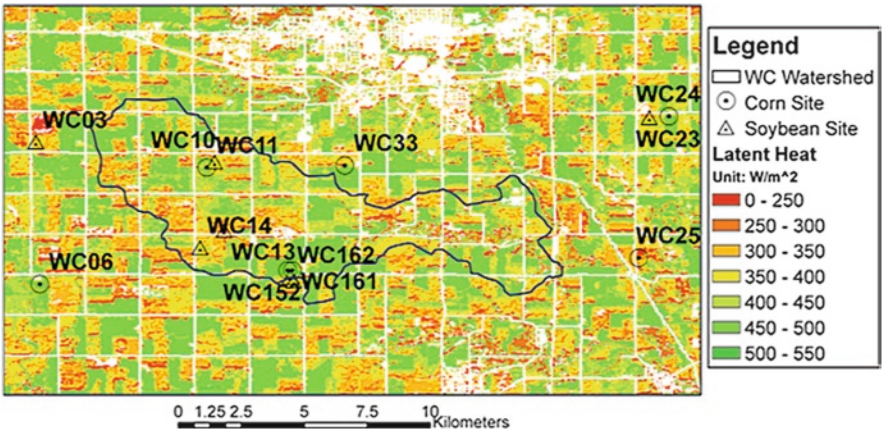

Fig. 33.2 Regional-scale evapotranspiration estimates from SEBS using a combination of Landsat surface temperature, MODIS emissivity, GOES radiation and NLDAS meteorological data

Table 33.2 SEBS data requirements for regional scale estimation of surface fluxes over the Walnut Creek catchment in Iowa, USA

Data source	Variables	Unit	Resolution
NLDAS	Air temperature	°C	0.125°
	Pressure	Pa	
	Wind	m/s	
	Specific humidity	–	
	Downward longwave radiation	W/m^2	
Landsat7 ETM+	Brightness temperature	K	60 m
	NDVI	–	30 m
	Land cover	–	30 m
MODIS	Albedo	–	1 km
GOES	Surface insolation	W/m^2	20 km

All inputs are based on operational meteorological and satellite data

NDVI data from the Landsat overpass (10:40 AM July 1, 2002 Path 26 Row 31) (Jackson and Cosh 2003b) were used. To maintain consistency, the 60-m surface temperature data were interpolated to 30 m using a nearest neighbor technique. Although interpolating the surface temperature is not strictly correct (due to non-linearity in the Planck function), it is not expected to introduce significant error at this scale (McCabe et al. 2008a). LAI and vegetation fraction were determined from the Landsat NDVI estimates using the experimentally derived nonlinear relationship of Xavier and Vettorazzi (2004).

The emissivity separation approach described above, along with vegetation fraction (f_v) knowledge, was used to calculate an effective emissivity (Chen et al. 2004). It is worth noting that the Landsat-based emissivity's higher spectral resolution is probably different from the tower surface temperature data, as the bandwidth (10.4–12.5 μm) is generally narrower than that of the infrared thermometer (8–14 μm).

Surface shortwave radiation data were determined from GOES-based estimates. The University of Wisconsin (pers. comm. Dr. M. C. Anderson 2004) provided the data for the study period at hourly time steps and a 20-km spatial resolution.

SEBS-Landsat-based estimates of the surface heat fluxes for July 1 (10:40 AM local time) were calculated for the SMACEX region using operational meteorological and ancillary remote sensing data. Figure 33.2 shows the latent heat flux estimates and the location of the flux tower sites over the catchment. A clear delineation between soybean and corn sites is immediately apparent.

To compare estimates with tower-based flux measurements, a 3 × 3 pixel box (90 m × 90 m) centered over each tower was extracted, and the mean latent flux estimate calculated. The results for SEBS-Landsat-based surface fluxes over both corn and soybean sites are presented in Table 33.3, identifying the mean, bias, and RMSE. Evapotranspiration estimates were assessed against eight flux tower sites, which were available for comparison on July 1. Table 33.3 indicates that the mean latent heat flux at corn sites is larger than at soybean sites, consistent with in-situ results. The latent heat flux difference between corn and soybean sites is approximately 120 W m^{-2} from in-situ observations and 92.0 W m^{-2} from SEBS-Landsat estimates. Individual RMS errors for corn and soybean were calculated as 28.7 and 84.9 W m^{-2} respectively, while the combined error for all sites was 60.6 W m^{-2}. Clearly, the results for soybean are not consistent with those for corn, with a large disparity in the retrieval accuracies. Analysis of the three soybean sites available for comparison reveals the influence of site WC161. WC161 is located adjacent to a cornfield. As a result, the 3 × 3 spatial averaging performed at this site will inevitably sample from within the higher evaporating corn site.

Comparing mean values of the latent heat fluxes determined from Landsat and those from the tower observations indicate improved agreement. For corn, the difference between the means of the SEBS-Landsat-based 3 × 3 estimates and the five corresponding tower values is less than 2%, whereas for the three soybean sites, it is approximately 5%. Although the results here indicate considerable agreement, the low number of validation points renders it difficult to draw broad conclusions on their accuracy at the local scale.

Table 33.3 Statistics of the surface energy flux comparison between SEBS-Landsat based estimation and in-situ tower based measurements for July 1, 2002

		Corn	Soybean	Corn and soybean
LE	Number of sites	5	3	8
	Observed mean (W/m^2)	459.3	339.9	414.6
	SEBS mean (W/m^2)	450.5	358.5	416.0
	Bias (W/m^2)	–8.8	18.6	1.4
	RMSE (W/m^2)	28.7	84.9	60.6
H	Number of sites	5	3	8
	Observed mean (W/m^2)	95.5	172.3	124.3
	SEBS mean (W/m^2)	81.2	111.2	92.5
	Bias (W/m^2)	–14.2	–61.0	–31.8
	RMSE (W/m^2)	23.8	86.3	60.0

The advantage of using remote sensing data is that spatial variability is analyzable explicitly and compared to point scale measurements. Figure 33.3 shows the results of the mean latent and sensible heat fluxes calculated for corn and soybean sites across the SMACEX domain, as well as the 3 × 3 pixel averages (see Table 33.3) compared with tower-based observations. To estimate the degree of spatial variability throughout the region, the range in flux tower measurements and the standard deviation of the SEBS-Landsat estimated fluxes across the region are also included. Generally, Fig. 33.3 shows that corn retrievals seem to agree more closely with observations than those for soybean, both for latent and sensible heat fluxes. Interestingly, soybean has an approximately 60% smaller standard deviation relative to corn in both surface fluxes, indicating greater flux consistency within soybean fields. The range of latent heat flux observations is approximately 65 W m^{-2} for corn and 100 W m^{-2} for soybean, although the latter result is again influenced by site WC161. Overall, the observations from the tower sites are seemingly representative of the regional average determined from the SEBS-Landsat results, but particularly so for corn. The variability of soybean results evident in Fig. 33.3 highlights the difficulty in characterizing flux measurements for large areas, even when good validation data are available for this purpose.

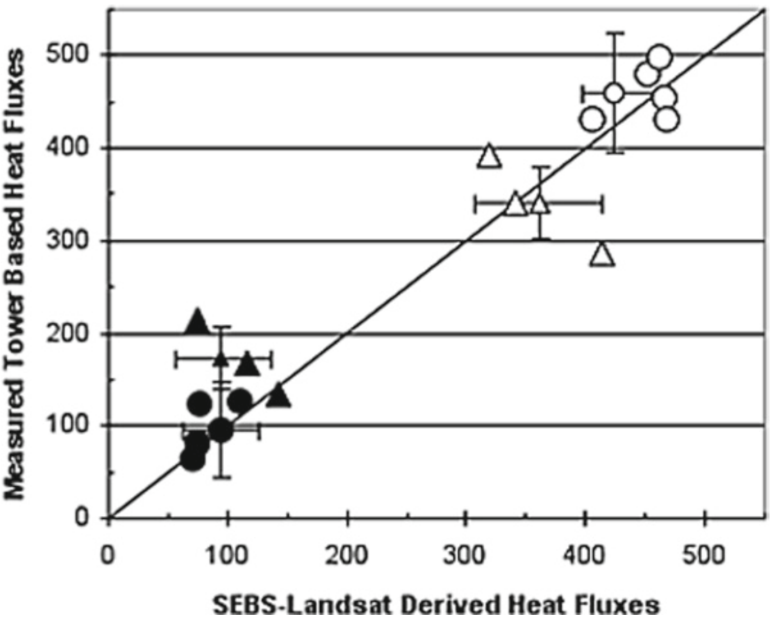

Fig. 33.3 Image is derived from Figure 4 in Su et al. (2005). Comparison of the energy fluxes from SEBS-Landsat-based estimates and in-situ observations at tower sites. *Circles* represent corn sites, while *triangles* signify soybean fields. *Solid symbols* identify the sensible heat flux and *open symbols*, the latent heat flux. The range of results present in tower observations are shown in the *x*-error bars and the standard deviation of satellite based estimates across the region in *y*-error bars. The regional average heat flux (across the domain) is shown at the intersection of these lines

33.3.1.3 Summary of Local- and Regional-Scale Validation

SEBS was evaluated at local and regional scales using both in-situ data and operational meteorology. Results from this analysis indicate that estimation accuracy was strongly related to crop type, with corn estimates showing improved estimates compared to soybean. Although RMSEs were affected by the limited number of samples and one poorly performing soybean site, differences between the mean observation values and SEBS-Landsat-based estimates at the tower sites were approximately 5%. Time-series comparison of the model output and observations also show that SEBS correctly interprets hydrological variability, and is capable of accurately representing the temporal development of evapotranspiration at the local scale. Using operational meteorological forcing data from the NLDAS offers an ideal pathway toward achieving robust estimates of regional-scale surface fluxes when coupled with remote sensing data. While the analysis here offers a retrospective determination of fluxes, the potential exists to employ such data at near real-time, allowing improved characterization of fluxes at time scales suitable for use in weather prediction, water resource management or agricultural applications. MODIS land product-derived surface parameters, GOES radiation information and NLDAS meteorological data form a sufficient database to run the SEBS model at a variety of scales. Combined with meteorological forcing from coarse scale operational data, flux estimates with considerable agreement with in-situ observations were producible.

Overall, these results indicate considerable potential toward routine surface heat flux estimation using remote sensing data and operational meteorology.

33.3.2 Globally Distributed Evapotranspiration Validation

The Coordinated Enhanced Observing Period (CEOP) forms an element of the World Climate Research Program (WCRP). Initiated as part of the Global Energy and Water Cycle Experiment (GEWEX), the CEOP dataset is ideal for SEBS validation requirements by providing continuous, high-quality in-situ measurements at global locations. The purpose of this case study is to assess the adaptability of SEBS to variations in climate and land cover based on the CEOP EOP-1 dataset at both tower and satellite pixel scales. Eight CEOP stations are selected to assess the SEBS model, specifically encompassing a variety of hydro-climatic conditions. An inter-comparison of energy fluxes from SEBS estimates and in-situ eddy correlation-based observations are examined at daily scales for each station.

Spatially representative in-situ data are often only available at a limited number of sites. To broaden the scope of the analysis and encompass a more operational approach to flux estimation, globally distributed forcing data are required. MODIS-based estimates of the land surface temperature and broadband emissivity, leaf area index and vegetation fraction are coupled with meteorology from both the CEOP towers and the Global Land Data Assimilation System (GLDAS) to formulate additional forcing datasets for SEBS. GLDAS is an integration of observational fields and outputs from the atmospheric data assimilation system (ADAS) component of a weather forecast and analysis system (Rodell et al. 2004), which provides data at 0.25° (spatial) and 3-h (temporal) resolutions. These distinct data sources allow a thorough examination of the impact to evapotranspiration estimates across two scales of meteorological forcing data. Further details of this work are provided in Su et al. (2007).

33.3.2.1 CEOP In-Situ Data and Site Characteristics

The Enhanced Observing Period (EOP-1) of CEOP provides hourly observation of surface meteorological variables and energy fluxes from July 1 through September 30, 2001. CEOP data provide the majority of the forcing variables required by SEBS. Excluding the Southern Great Plains site, eight stations (six sites) from EOP-1 meet the data requirements of the SEBS model, with site names and characteristics (i.e., country, location, land classification and climate type) listed in Table 33.4. The six sites are distributed across five countries and three continents, and fall into three broad climate types and four different vegetation covers. The data include three forested locations within the Boreal Ecosystem Research and Monitoring Sites (BERMS). For CEOP tower-based forcings, surface temperature observations were only available at Bondville and Rondonia. For locations where the surface temperature is not observed directly, it is estimated indirectly from the upward and downward longwave radiation using a correction for the broadband emissivity.

33.3.2.2 Results from the Globally Distributed Tower-Based Flux Data

Daily averages (05:00 through 18:00 local time) and statistics for the energy fluxes at eight globally distributed CEOP stations are presented in Table 33.5. To filter out periods of cloud-affected or rainy days, the daily average is computed only for

Table 33.4 Characteristics of the CEOP-EOP1 reference sites

Site name	Country	Lat./lon. (°)	Köppen climate	Dominant land cover (DLC)
Cabauw	Netherlands	51.97, 4.93	C	Grassland
Lindenberg	Germany	52.17, 14.12	C	Grassland
Bondville	USA	40.01, –88.29	D	Cropland (corn)
Rondonia	Brazil	–10.01, –61.93	A	Rain forest
Manaus	Brazil	–2.61, –60.21	A	Rain forest
BERMS sites				
Old Aspen	Canada	53.63, –106.20	D	Forest
Old Jack Pine	Canada	53.92, –104.69	D	Forest
Old Black Spruce	Canada	53.99, –105.12	D	Forest

A: tropical; B: dry; C: warm temperate rainy climates and mild winters; D: cold forest climates and severe winters; E: polar; H: highland

Table 33.5 Statistics of the daytime latent heat flux and evaporative fraction at the daily scale for the CEOP globally distributed locations

Site name	Days	Mean CEOP LE (W/m^2)	Mean SEBS LE (W/m^2)	RMSE SEBS LE (W/m^2)	r-RMSE SEBS LE (%)	Mean EF CEOP	Mean EF SEBS
Cabauw	45	146.47	144.54	30.20	20.62	0.756	0.708
Lindenberg	70	119.49	102.70	22.61	18.92	0.741	0.625
Bondville	23	299.68	293.85	74.17	24.75	0.602	0.582
Rondonia	66	226.45	235.73	40.58	17.92	0.725	0.672
Manaus	31	318.85	344.16	50.89	15.96	0.758	0.787
BERMS							
Old Aspen	84	151.09	122.80	48.25	31.93	0.548	0.576
Old Jack Pine	76	101.50	106.80	29.28	28.85	0.315	0.278
Old Black Spruce	62	134.68	118.55	56.78	42.16	0.362	0.402

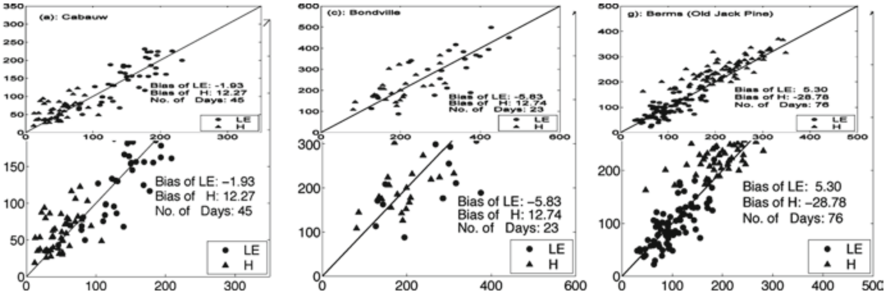

Fig. 33.4 Comparison of daily average SEBS flux estimates using CEOP forcing data and MODIS retrievals compared with measured fluxes at the CEOP observation sites. Both axes represent surface heat flux with units of W m^{-2}

periods when both the observations, and the model estimates are available for more than 4 h/day. Three representative sites are shown for comparison in Fig. 33.4. RMSE estimates of the daily flux indicate a varied level of agreement across the CEOP sites. Considering the range of RMSE and mean flux values, flux results require some normalization to allow intercomparison. The relative RMSE (r-RMSE) was calculated by dividing the RMSE by the mean observed flux as a way to assess the accuracy of SEBS estimates. Based on the relative RMSE, the tropical rain forest sites at Manaus and Rondonia (Brazil) represent the highest accuracy (<20% r-RMSE), followed closely by the two grassland sites at Lindenberg and Cabauw (~20% r-RMSE). The cropland site (corn) at Bondville presents good agreement given the uncertainty in land classification here (~25% r-RMSE), whereas the remaining forested sites illustrate the largest uncertainty and varied levels of agreement (>25% r-RMSE).

The comparison of the mean evaporative fraction (evaporation divided by available energy) shows that estimates from SEBS agree very well with those from observations and exhibit no significant bias. Both model-predicted and observed mean evaporative fractions at the two tropical sites are above 0.65 during the summer of 2001, which is reasonable considering the climatic conditions in the Amazon, where water supply is sufficient for sustained forest growth. Cabauw and Lindenberg also have a high-observed mean evaporative fraction in summer. For the Cabauw grass site, the soil is reported to exist at field capacity for much of the year, thus evaporation is seldom limited by the water supply (Chen et al. 1997). The largest difference in mean EF is 0.111 at Lindenberg. Generally, the SEBS evaporative fraction estimate illustrates a close agreement with that from observations.

These results illustrate that both climate and vegetation type have an important control over the daytime surface heat flux patterns. The SEBS model is observed to reproduce the patterns of the daily surface heat flux under diverse climate conditions and vegetation types. While the SEBS sensible and latent heat flux estimates for the Boreal forests are not as accurately reproduced, such vegetated stands represent some of the most difficult surface types to model evapotranspiration, due to their strong coupling with the atmosphere (Margolis and Ryan 1997) and uncertainties in retrieving required variables. In the majority of studies cases, estimates of the daytime evapotranspiration agree within an r-RMSE of approximately 30%.

33.3.2.3 Results from MODIS-CEOP and MODIS-GLDAS Derived Fluxes

Evapotranspiration estimates were produced at 1-km resolution using both CEOP and GLDAS forcing data coupled with MODIS land surface temperature (MOD11A1) (Table 33.6). The surface meteorological and radiative data in both CEOP and GLDAS forcing were interpolated to correspond with the overpass time of the MODIS surface temperature data. When remotely sensed data are incorporated, model-predicted evapotranspiration is limited not only by meteorological forcing data, but also by the MODIS surface temperature availability, which is strongly influenced by cloud cover and atmospheric influences. Three sites, which most consistently derive evapotranspiration, are presented for comparison between SEBS-based estimates and tower scale CEOP observations.

Scatter plots comparing MODIS-based retrievals with in-situ flux measurements are shown in Fig. 33.5. As mentioned in the previous section, both meteorological data and surface heat flux measurements were linearly interpolated to correspond

Table 33.6 Forcing data for globally distributed evapotranspiration estimates

Data source	Variables	Spatial resolution	Temporal resolution
CEOP	Surface meteorology	Tower scale	Instantaneous, interpolated
GLDAS	Surface meteorology	0.25°	Instantaneous, interpolated
MODIS	LST/emissivity	1 km	Instantaneous
	LAI		8-day
	Land cover		Yearly
	Albedo		16-day

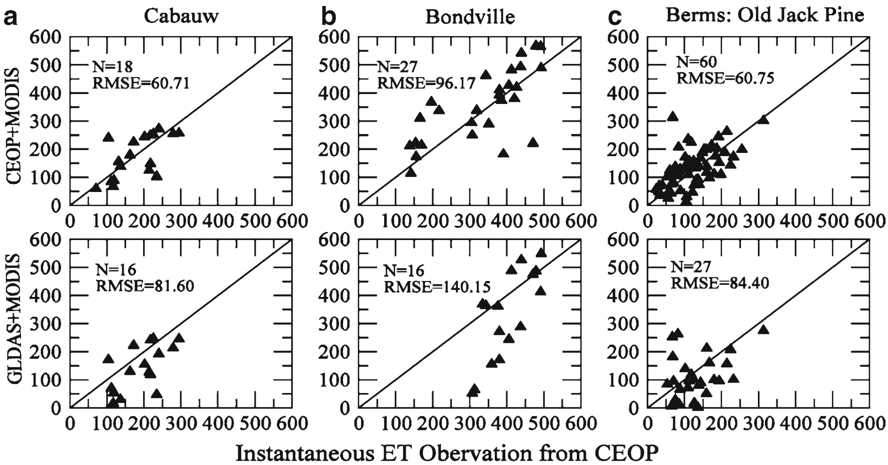

Fig. 33.5 Comparison of instantaneous SEBS evapotranspiration using CEOP meteorological data (*top*) and GLDAS forcing data (*bottom*) together with MODIS retrievals. Values on the x-axis are determined from CEOP tower based observations of surface fluxes (W m^{-2})

with the MODIS overpass time at each site. The number of available model estimates and the RMSE are included in each panel. The three sites represent quite different land classifications, including grassland, cropland and cold forest, respectively. A greater number of estimates were obtained from the CEOP+MODIS dataset than from GLDAS+MODIS dataset, although they share the same remotely sensed land surface parameters. Likewise, for all three sites, the evapotranspiration accuracy estimates from CEOP+MODIS dataset are better than those from the GLDAS+MODIS dataset. Specifically, the results from CEOP+MODIS dataset have less bias, less MAE, and less RMSE. This result is not unexpected considering GLDAS meteorological forcing represents a coarser spatial and temporal resolution (0.25° and 3 hourly); however, it is instructive given the option of using global operational forcing.

The RMSE of surface flux estimates at Cabauw and BERMS (old Jack Pine) based on CEOP+MODIS dataset is around 61 W m^{-2}, while results for Bondville indicate an RMSE of 96.17 W m^{-2}. The RMSE of latent heat flux estimates are higher by approximately 33% at Cabauw and BERMS when CEOP forcing is replaced with the GLDAS forcing dataset. For Bondville, the increase in error approaches 45%. These results raise some potential limitations to the broad scale estimation of surface fluxes using globally distributed operational forcing datasets.

33.3.2.4 Summary of Globally Distributed Evapotranspiration Validation

Several factors can potentially affect the accuracy of model-predicted energy fluxes. When combined with remote sensing data, the lack of temporal detail available from measures such as the surface temperature (daily) and LAI (8-day), influence the capacity to capture the dynamics of the evaporating surface, particularly over complex landscapes and growing conditions. From previous analysis, the evaporative fraction was observed to increase from 0.50 to 0.90 within 3 weeks during a period of rapid growth. Figure 1 in Su et al. (2007) demonstrate the variability of LAI during EOP-1 and the subsequent difficulty in effectively capturing these dynamics. Scale issues are another important factor requiring consideration. MODIS land cover classification data at 1-km lacks the degree of variability necessary to correctly parameterize detailed land surface models, or even process models such as SEBS. McCabe and Wood (2006) demonstrated the degree of error resulting from misclassification of known surface types.

The poor performance of the Bondville site is explained to a large degree by land surface heterogeneity effects. Although characterized as a corn crop, Bondville is actually a mixture of corn and soybean within the 1-km MODIS pixel since the two stations at Bondville (which are 400 m apart) were planted with opposite crops (corn and soybean) in 2001 (information from http://www.fluxnet.ornl.gov/fluxnet/index.cfm). Su et al. (2005) found that corn routinely exhibits an evapotranspiration up to 100 W m^{-2} greater than for soybean. Thus the heterogeneity within a MODIS pixel would certainly account for the relatively large deviation of evapotranspiration estimates at Bondville evident in all three forcing datasets.

While land surface misclassification may explain aspects of the error, variations in forcing data can potentially contribute much larger sources of inaccuracy. Examination of net radiation from the GLDAS and comparison with CEOP data indicated considerable divergence at all sites presented here. Amongst these, Bondville has the largest negative bias for incoming shortwave (160.1 W m^{-2}), more than twice the bias at the other sites. The poorer surface flux estimates at Bondville and Cabauw are certainly attributable to the large error in the GLDAS downward radiative forcing, given the strong reliance of evapotranspiration on accuracy in available energy (Rn-G).

Forcing data sources such as GLDAS offer immediate advantages, but their use requires prudence especially in areas with limited validation data.

33.4 Application with EOS-Terra and Aqua Data

Techniques which couple land and atmospheric properties' information with remotely sensed variables offer considerable promise to routinely retrieve a number of hydrological variables. Over the last few decades, much effort was directed toward determining evapotranspiration and its spatial variability. Understanding the limitations of remote sensing approaches is as important as identifying their possibilities. Using space-borne remote sensing to estimate surface evapotranspiration at regional to continental scales with algorithms based on micrometeorological approaches present a number of unique challenges. The main challenges include the following: (1) obtaining continuous surface temperature fields uninhibited by clouds; (2) errors in transferring the required surface meteorology from in-situ stations to pixels with retrieved surface temperatures; (3) scale mismatches between the resolution of the remotely sensed observations (insolation, vegetation, surface temperature); (4) natural landscape variability; and (5) aggregating instantaneous surface flux estimates spatially and temporally across large domains.

Despite restrictions associated with atmospheric influences, land surface heterogeneity, the overpass frequency and the development of robust process algorithms, satellite-derived data remain the only viable means to measure evapotranspiration at regional and larger scales on a routine basis. A key concept underpinning the development of a MODIS-based evapotranspiration estimate is to develop a globally distributed product based on local scale evaluation. To achieve this task, a deliberate modeling and evaluation phase is developed, which incorporates multiple sensors, scales and land surface types to assess the feasibility to routinely estimate evapotranspiration. Much of the work and progress toward such a product are available in recent publications, which include Su et al. (2005, 2007), McCabe and Wood (2006), and McCabe et al. (2008b).

The following section describes a recent case study that illustrates an approach using a combination of in-situ and remote sensing datasets to estimate distributed patterns of evapotranspiration across the Oklahoma Mesonet.

33.4.1 Regional- to Continental-Scale Investigations Using the Oklahoma Mesonet

The work presented here uses Terra and Aqua MODIS products, together with a medium spatial resolution (5 km) surface solar insolation product derived from the MODIS sensor (Pinker et al. 2003; Su et al. 2008). The strategies explored in this study form a baseline to assess MODIS-based evapotranspiration at regional to continental scales.

In this study, SEBS is employed to estimate the terrestrial evapotranspiration across Oklahoma state using a combination of remote sensing and in-situ data. The Oklahoma Mesonet (see http://www.mesonet.org/) provides an unprecedented level of meteorological detail over portions of the Red-Arkansas basin, a 645,000 km^2 sub-catchment of the continental-scale Mississippi Basin. The Mesonet consists of over 120 towers that deliver needed surface and atmospheric variables such as air temperature, relative humidity, pressure, wind speed, and downward shortwave radiation (insolation) at 5-min intervals.

A number of strategies are explored to obtain continuous spatial fields of evapotranspiration. An inverse distance weighting interpolation scheme is used to produce spatially continuous fields of surface meteorology based on available tower data. This enables a streamlined integration with grid-based remote sensing data, and provides the necessary spatial forcing data required by SEBS. Comparisons of interpolated in-situ measurements of incoming shortwave (solar) radiation with a MODIS-derived incoming shortwave radiation product are examined, and these data are used for subsequent model simulation. Figure 33.6 presents a spatial comparison of the incoming solar radiation field from interpolated tower data and Aqua MODIS data.

Different combinations of these data fields were inter-compared to assess the evapotranspiration retrieval's fidelity in an operational context. SEBS was also used to predict the evaporative fraction over individual operational meteorological stations, with values then interpolated across the domain to provide a spatial evaporative fraction field. In all, three unique experiments combining the different levels of forcing data (both in-situ and remote) were developed. Table 33.7 shows the experimental design and the forcing combinations.

Scatter plots of Experiments II and III compared with the tower-based retrievals of Experiment I for both Terra and Aqua overpasses are presented in Fig. 33.7. A comparison of these experiment results reveals the following: when the interpolated downward shortwave radiation at the tower sites (Experiment II) is substituted with the corresponding MODIS-based shortwave radiation (Experiment III), the standard deviation of evapotranspiration is 7–0 W m^{-2} lower than when compared against the tower-based results in Experiment I. The result is consistent across both Terra and Aqua overpasses, which suggests that incorporating MODIS-based downward shortwave radiation results is beneficial to improve evapotranspiration estimation, particularly when no regional in-situ measurements of this variable are available.

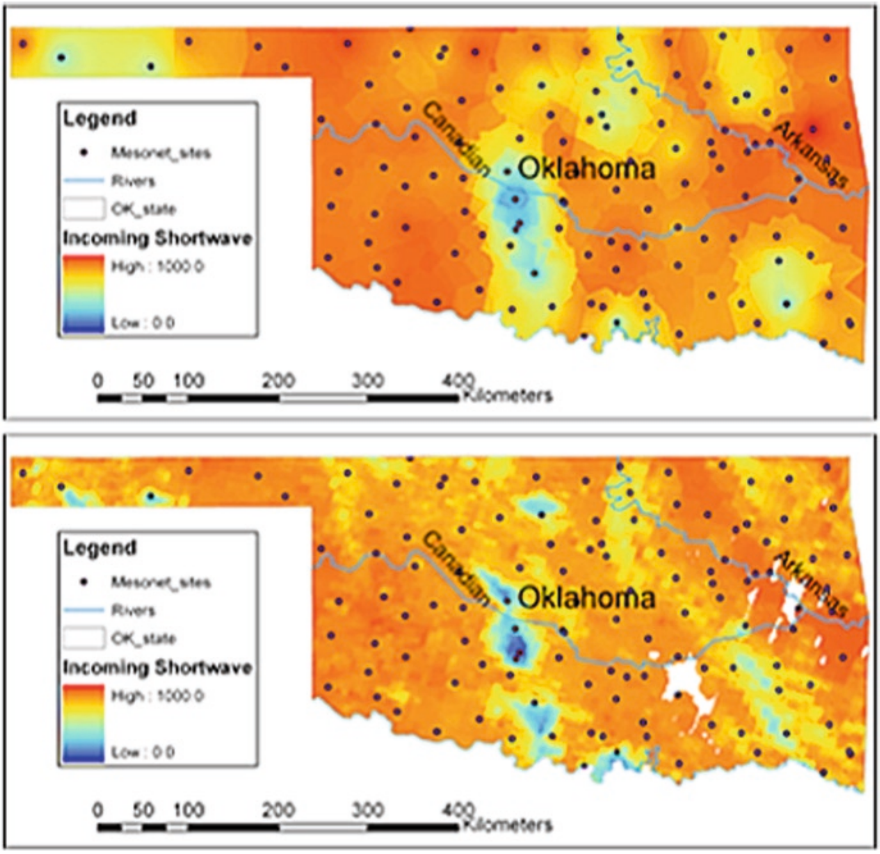

Fig. 33.6 Incoming shortwave radiation in W m^{-2} from gridded Oklahoma Mesonet surface meteorology (*upper*) and derived from MODIS-Aqua (*lower*) for August 8, 2003

Table 33.7 Description of the three individual experiments developed for the Oklahoma Mesonet analysis to assess the retrieval of spatially distributed evapotranspiration

Experiment	Data source and methodology
I	Mesonet in-situ tower data (air temperature, relative humidity, pressure, wind speed and downward shortwave radiation) and MODIS derived land surface temperature, leaf area index and albedo
II	Interpolated Mesonet in-situ tower data (see Experiment I) and MODIS derived land surface temperature, leaf area index and albedo
III	Interpolated Mesonet in-situ tower data (see Experiment I) but using MODIS derived downward shortwave radiation together with MODIS land surface temperature, leaf area index and albedo

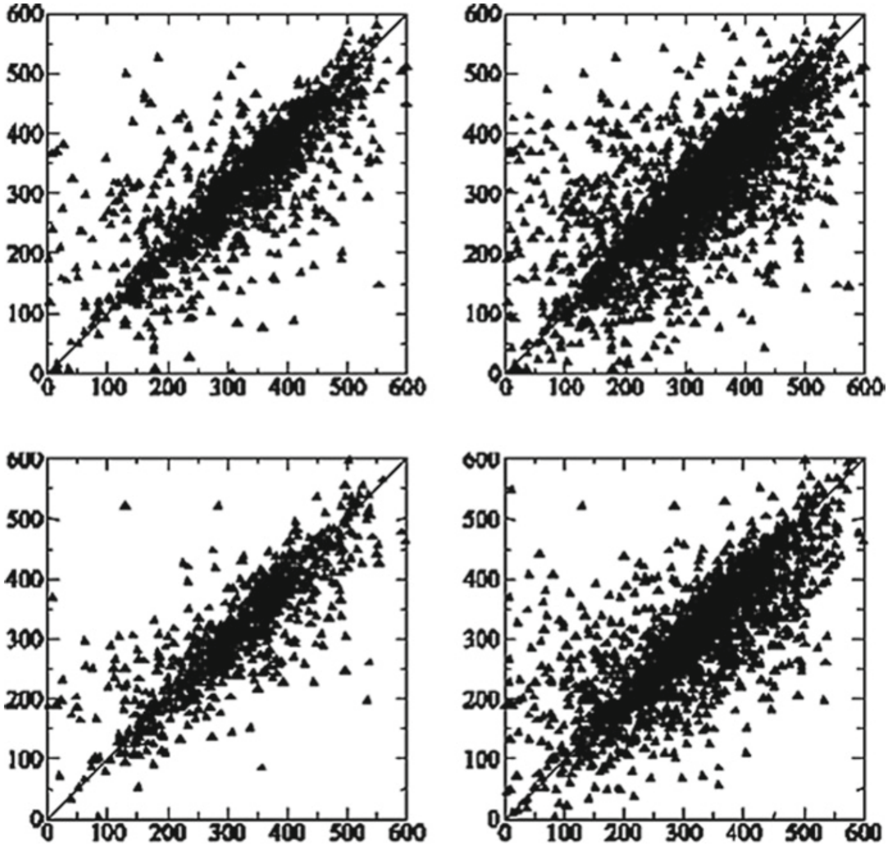

Fig. 33.7 Scatter plots comparing Experiments II and III (refer to Table 33.7) with SEBS latent heat flux derived from Mesonet tower observations (Experiment I) for Terra (*left column*) and Aqua (*right column*)

In both Experiments II and III, Terra results improve when compared against Aqua (and relative to the in-situ tower-based retrievals). Such improvement is likely a function of interpolating meteorological fields at different points in the diurnal cycle. This is explainable thus: the afternoon Aqua overpass will generally exhibit more spatial variability than the earlier morning Terra overpass, purely as a result of solar and atmospheric forcing at those times.

Spatial maps of the evapotranspiration and the evaporative fraction (evapotranspiration divided by the available energy) were determined for a 10-day period over Oklahoma. It was necessary to average daily measurements to the 10-day period due to the relatively poor retrieval rate of surface temperature during the study period. Indeed, this is one of the critical limitations in developing a temperature-based evapotranspiration product: the limitation due to cloud cover variability to produce a continuous spatial field. Composites of spatial evapotranspiration for the first 10 days of August 2003 are shown in Fig. 33.8 for both Terra and Aqua using the results from Experiments II and III.

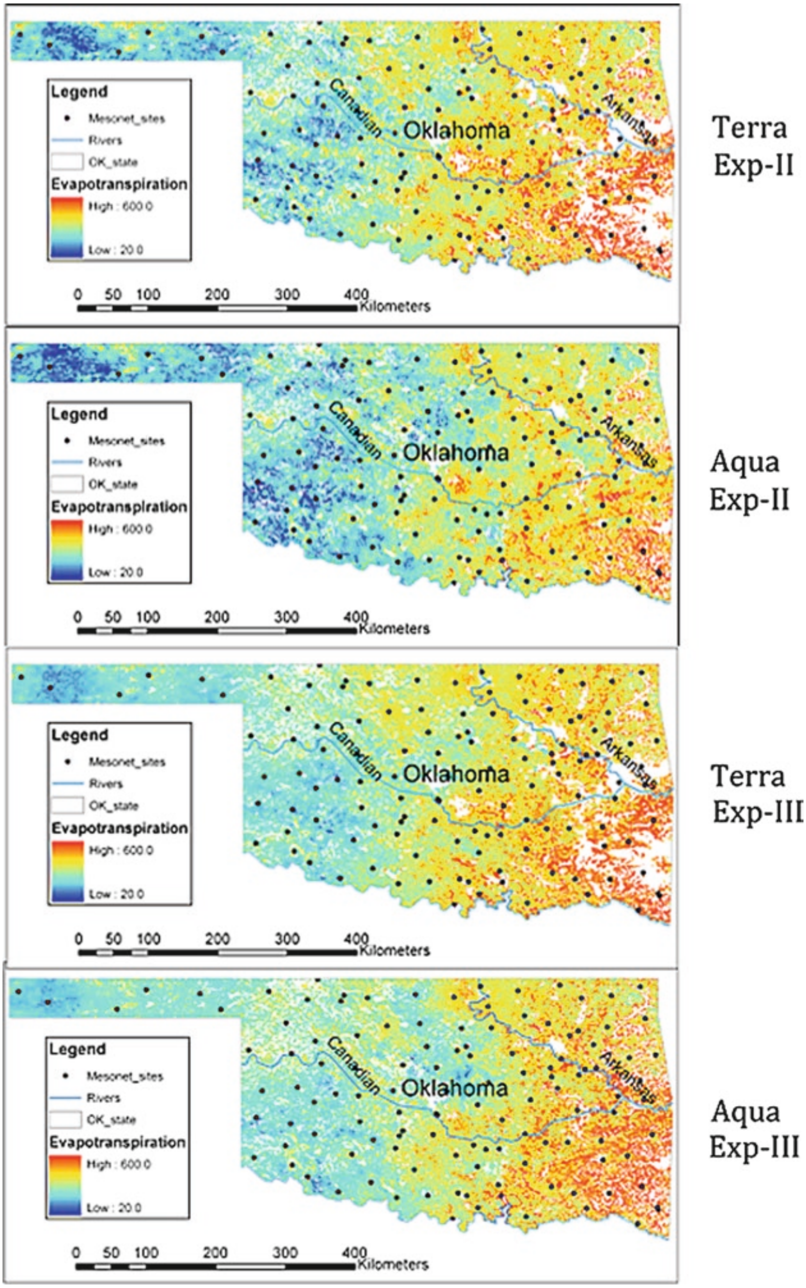

Fig. 33.8 Composite model output for 10-day modeled evapotranspiration between August 1–10, 2003 from the MODIS-Terra and MODIS-Aqua for both Experiment II (*top*) and Experiment III (*bottom*) (refer to Table 33.7 for explanation of forcing data). Flux estimates are in W m^{-2}

Evidently, there is a high level of agreement among the spatial maps derived from individual sensor retrievals, indicating a potential to develop a combined Terra+Aqua product to circumvent the cloud contamination issues of the 5-km product. However, the significant surface temperature changes that occur between Terra and Aqua overpasses could potentially affect such a product's accuracy. The 0.05° land surface temperature climate modeling grid (CMG) product shows some improvement in cloud screening, and may provide an alternative approach to temperature retrieval. Further work on this is required.

33.4.2 Developing a Multisensor Approach Toward Global Estimation

In the preliminary stages of developing a MODIS-based evapotranspiration product, the SEBS approach was deemed usable in concert with available surface meteorological fields, supplemented with remote sensing data. As part of this task, the efficacy of using model forcing and ground-based data, as well as the accuracy of retrievals, was undertaken. During the first 2 years of the project, SEBS was evaluated using flux tower data from SMACEX 02 (Iowa) and GEWEX/CEOP EOP-1 tower data. Where good quality data exist, the results were excellent and were reported by Su et al. (2005, 2007). Assessment of the algorithm continues using FLUXNET data (http://daac.ornl.gov/FLUXNET/). The project also began testing the SEBS algorithm over two large regional scales: the Red-Arkansas river basin, and over Arizona during the North American Monsoon Experiment (NAME) field campaign period (see McCabe et al. 2008b; Pan et al. 2008).

Through analyses of both the evapotranspiration and SEBS-required forcing data to retrieve evapotranspiration, it was clear that there were deficiencies in predicating the surface flux product solely on MODIS data. Apart from known issues in the surface temperature and vegetation products (retrieval frequency, accuracy, and dynamic response), another primary concern was the lack of a MODIS-based solar radiation product. To address this lack, collaborative work with the University of Maryland (Pinker et al. 2003) helped develop a MODIS-based radiation product, which produced excellent results to assess over Oklahoma (Su et al. 2008).

More recent efforts were directed toward using complementary sensors on-board the Terra and Aqua satellites: in particular, the Cloud and the Earth Radiant Energy System (CERES) for radiation components and surface temperature, and the Atmospheric Infrared Sounder (AIRS) for surface air temperature and humidity. These sensors provide a means to develop a truly global scale product, since the in-situ meteorological variables required by SEBS are not routinely available globally. Figure 33.9 shows some of the swath-based retrievals of the variables used by SEBS to estimate evapotranspiration.

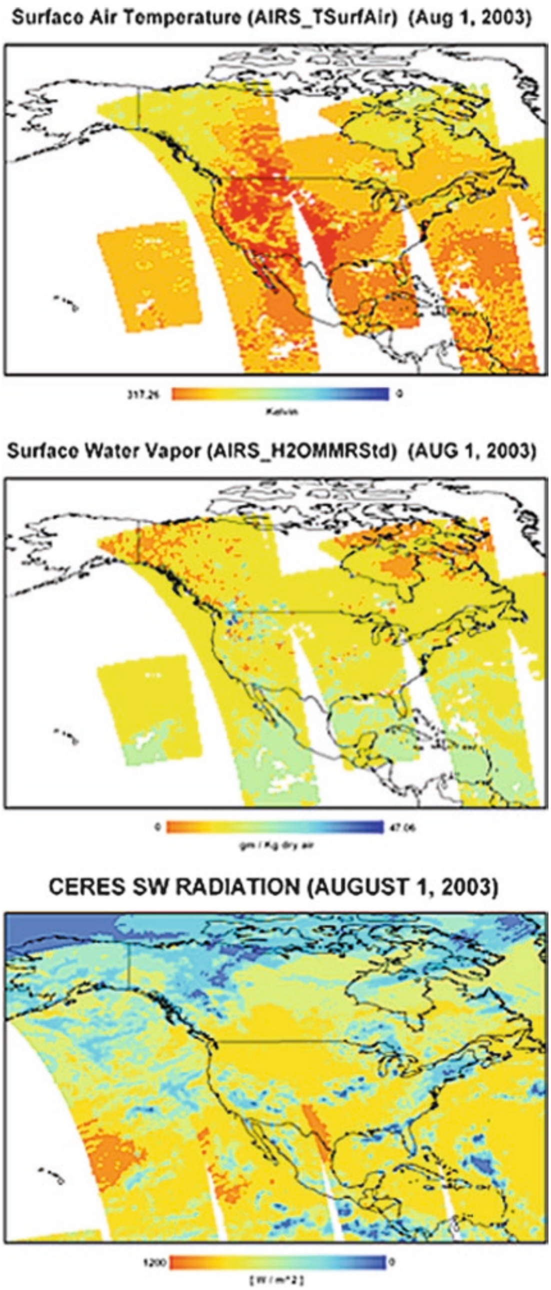

Fig. 33.9 Examples of swath data derived from AIRS and CERES including (from *top*) AIRS surface air temperature, AIRS surface water vapor and CERES shortwave radiation for August 1, 2003

These efforts to augment the MODIS data with both AIRS and CERES products have produced some positive results, some of which are presented in Fig. 33.10 for Oklahoma using combinations of AIRS meteorology, MODIS-based radiation and surface temperature, and finally, CERES-based radiation and surface temperature. As is evident, there are significant spatial resolution differences in using only MODIS data (1–5 km) in comparison with CERES and AIRS data (20 and 25 km, respectively), but the spatial patterns are well correlated. Table 33.8 shows the list of some of the data sources that drive the current progress to develop a globally distributed evapotranspiration product.

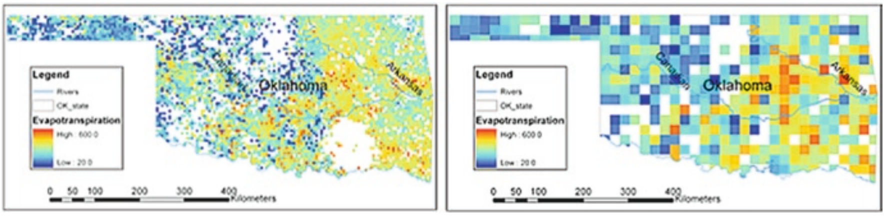

Fig. 33.10 Retrieved evapotranspiration over Oklahoma using (*left panel*) MODIS land products, MODIS radiation and AIRS meteorology and (*right panel*) CERES radiation and LST, AIRS meteorology and MODIS land products

Table 33.8 Data types and sources for the development of a multisensor evapotranspiration product

Data type	Variable	Unit	Source	Platform	Resolution (km)
Surface meteorological data	Air temperature	°C	AIRS	AQUA	25[a]
	Pressure	kPa	AIRS	AQUA	25[a]
	U-Wind	m/s	(GMAO/CERES)	AQUA	20
	V-Wind	m/s	(GMAO/CERES)	AQUA	20
	Vapor pressure	kPa	AIRS	AQUA	25[a]
Radiative energy flux	Incident SW	W/m^2	CERES	AQUA	20
	Incident LW	W/m^2	CERES	AQUA	20
	Surface temperature	°C	CERES/AIRS	AQUA	20/25
Vegetation Parameters	Emissivity	–	MODIS	AQUA	1–5
	Albedo	–	MODIS	AQUA	5
	LAI	–	MODIS	AQUA	5
	Veg. type	–	MODIS	AQUA	1–5
	(MODIS UMD Classification)	–	MODIS	TERRA	20

[a]Processed to 25 km at Princeton

33.5 Current Status and Future Direction

33.5.1 Problems and Issues in Remote Retrievals

General sentiment agrees that remote sensing offers the most amenable means to obtain spatial evapotranspiration patterns. But, there exists little agreement on how best to realize this. While numerous schemes and methodologies were proposed to provide land surface flux estimates with remotely sensed surface temperatures (Diak and Whipple 1995; Anderson et al. 1997; Norman et al. 2000), evapotranspiration estimates derived in such a fashion have achieved varied success levels. Undoubtedly, accurate measurement of surface fluxes with remote sensing techniques would provide a valuable information source, and much progress was made toward achieving this goal (Kustas and Norman 1997; Norman et al. 2003; Kalma et al. 2008).

The SEBS model has demonstrated its ability to produce accurate surface heat flux estimates over agricultural fields using both in-situ and NLDAS-based observational meteorological forcing (Su et al. 2005); globally distributed sites representing disparate land surface types and conditions (Su et al. 2007); and more recently, with MODIS-based radiation and NLDAS forcing over a large basin in the USA. An analysis of scale influence using multisensor remote sensing data was also performed and showed the utility of MODIS retrievals to develop good estimates of the catchment average evapotranspiration (McCabe and Wood 2006). The clearest message from these evaluations is the self-evident conclusion that quality evapotranspiration estimates are only obtained with quality forcing data and remote sensing data.

Excluding the availability of needed forcing data, which is increasingly met by operational meteorological forcing, a critical limitation to routine evapotranspiration estimation is the provision of surface temperature measurements. Accurate retrieval of land surface temperature is difficult due to a number of underlying factors, which combine to provide some interesting challenges. Sea surface temperature retrievals are potentially accurate in the order of 1 K (Prata et al. 1995), but surface temperature estimates are complicated by spatial and temporal resolution, land surface heterogeneity and atmospheric and land surface effects. Coupled with the inability of infrared techniques to penetrate cloud-covered pixels, obtaining spatially continuous surface temperature fields is rare. Cloud presence also increases the radiative flux variations reaching the surface, which renders attempts to extrapolate instantaneous evapotranspiration estimates either spatially (through interpolation) or temporally (through consistency relationships with the evaporative fraction e.g., Crago 1996) difficult.

Another problem in accurate surface flux estimation is the accuracy of land cover classification, fractional vegetation cover and leaf area index – all products derived from MODIS data. Surface flux retrievals are significantly influenced by correct specification of vegetation properties, and issues related to capturing the dynamic response in vegetation systems (particularly LAI) are observed in field and regional-scale analysis. This issue is of particular concern over regions of the globe, which are not thoroughly validated, or lack the means to perform effective product evaluation. As with surface temperature, the scale issue becomes significant, especially in heterogeneous environments and where mixed land-use occurs.

Characterizing the development of evapotranspiration through time is a difficult task, particularly when using remote sensing data, since retrieved information is often spatially dense, but temporally sparse. Techniques to expand these instantaneous measures are not only limited, they are restricted by the general lack of knowledge to effectively describe the spatial distribution and temporal evolution of evaporative patterns. Although advances in providing accurate evapotranspiration estimates from remote sensing variables are noted and evidenced herein, one of the major shortcomings of such techniques is their basis rooted on essentially instantaneous retrievals. Approaches, which use snapshots of the surface condition to expand surface flux knowledge through time, show much promise. Recent techniques that address this issue include the use of uncertainty modeling (McCabe et al. 2005), multi-objective calibration (Crow et al. 2004) and data assimilation schemes that account for multiple hydrological observations (Pan et al. 2008).

Problems of correct process representation, accounting for uncertainties due to scale and heterogeneity, or characterizing errors in forcing data and their influence on model estimates are not the only issues, which require resolution. Perhaps the key obstacle toward achieving robust and accurate evapotranspiration estimates at globally distributed locations is the lack of quality validation data. Indeed, this leads to a serious shortcoming in remote sensing observations per se; there is a distinct lack of validation data characterizing a wide variety of surface and atmospheric states against which techniques are robustly assessed. Recent efforts addressing the ideas of hydrological consistency (McCabe et al. 2008b) or research to find statistical consistency with land surface model data (Gao et al. 2007) offer some promise toward challenging the current validation–evaluation paradigm.

33.5.2 Future Directions

The development of a global evapotranspiration product demands the successful integration of multiple satellites and sensors. The current availability of EOS represents a rare opportunity to examine the efficacy to incorporate these multiple data into an interpretive process model (SEBS) to allow characterization of needed hydrological and climatological variables. The planned shift in research strategy moves away from a reliance on ground-based meteorology toward a combination of observations from MODIS, CERES and AIRS sensors that will enable global retrievals at mid-level resolution. Preliminary analysis of these data suggests a significant advantage over reliance on single sensor estimation. An initial global-scale evapotranspiration retrieval using these multiple data sources is presented in Fig. 33.11. The result represents the successful evolution of much of the

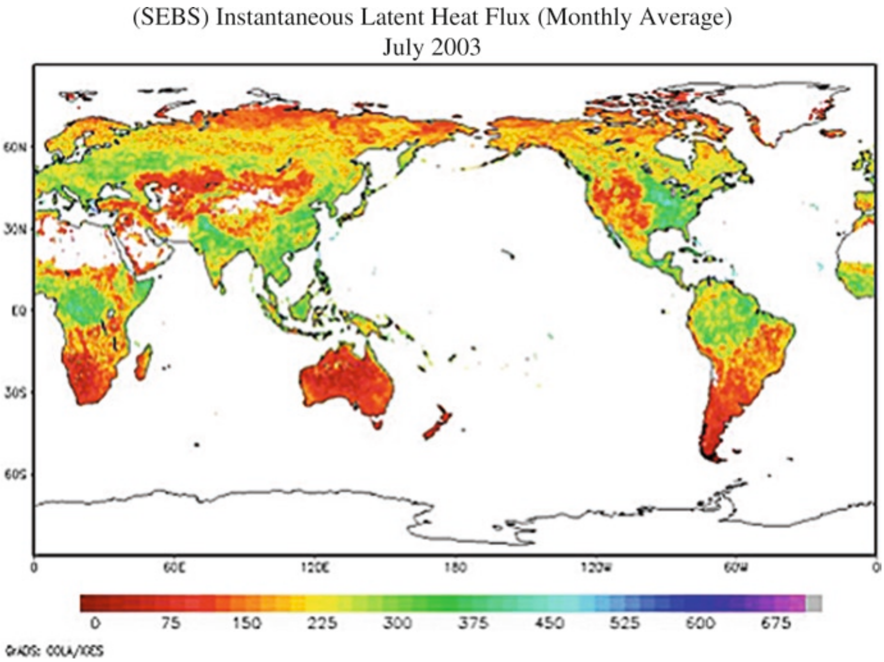

Fig. 33.11 Preliminary results for a new global estimate of evapotranspiration using SEBS and combinations of MODIS, AIRS and CERES data for July 2003 (W m^{-2})

work presented in this chapter and offers a means to produce routine global evapotranspiration estimates.

One of the key issues that require attention is the manner in which evapotranspiration evaluation should proceed. While studies have shown the stability and accuracy of the interpretive model (SEBS) to estimate surface fluxes with good quality data, the different retrieval scales inherent in a global product will demand some innovation in product assessment. Studies examining the hydrological consistency of remotely sensed hydrological variables were undertaken (McCabe et al. 2008b), and work continues over continental scales and longer time periods to examine this approach. Additionally, comparison with land surface model outputs and data assimilation studies to address the added skill from remote observations may also provide a needed means of assessment. Research also continues to examine atmospheric water budgets based on re-analysis divergence fields, and observed precipitation to provide a more accurate characterization of water budget closure. Together with comparison with spatially distributed tower data available at selected locations globally, this represents a comprehensive assessment strategy that should offer some confidence in remote sensing-derived evapotranspiration retrieval.

Acknowledgments NASA supported this work through grant NNG04GQ32G: A Terrestrial Evaporation Product Using MODIS Data. This support is gratefully acknowledged.

References

Allen RG, Tasumi M, Trezza R (2007) Satellite-based energy balance for mapping evapotranspiration with internalized calibration (METRIC): applications. ASCE J Irrigation Drainage Eng 133(4):395–406

Anderson MC, Norman JM, Diak GR, Kustas WP, Mecikalski JR (1997) A two-source time-integrated model for estimating surface fluxes using thermal infrared remote sensing. Rem Sens Environ 60(2):195–216

Anderson MC, Norman JM, Mecikalski JR, Otkin JA, Kustas WP (2007) A climatological study of evapotranspiration and moisture stress across the continental United States based on thermal remote sensing: 1 Model formulation. J Geophys Res 112:D10117, doi:10.1029/2006JD007506

Bastiaanssen WGM, Pelgrum H, Wang J, Ma Y, Moreno JF, Roerink GJ, Van der Wal T (1998) A remote sensing surface energy balance algorithm for land (SEBAL): 2 Validation. J Hydrol 212/213:213–229

Beven KJ, Fisher J (1996) Remote sensing and scaling in hydrology. In Stewart JB, Engman ET, Feddes RA, Kerr Y (eds) Scaling up in hydrology using remote sensing. Wiley, Chichester, UK

Bisht G, Venturini V, Islam, S, Jiang L (2005) Estimation of net radiation using MODIS-Terra data for clear sky days. Rem Sens Environ 97(1):52–67

Brunsell NA, Ham JM, Owensby CE (2008) Assessing the multi-resolution information content of remotely sensed variables and elevation for evapotranspiration in a tall-grass prairie environment. Rem Sens Environ 112:2977–2987

Chen JM, Cihlar J (1995) Quantifying the effect of canopy architecture on optical measurements of leaf area index using two gap size methods. IEEE Trans Geosci Remote Sens 33:777–787

Chen LF, Li Z-L, Liu S, Tang Y, Zhong B (2004) Definition of component effective emissivity for heterogeneous and non-isothermal surfaces and its approximate calculation. Int J Remote Sens 25:231–244

Chen TH and Coauthors (1997) Cabauw experimental results from the Project for Intercomparison of Land-surface Parameterization Schemes. J. Climate, 10:1194–1215

Crago RD (1996) Conservation and variability of the evaporative fraction during the daytime. J Hydrology 180(1–4):173–194

Crow W, Wood EF, Pan M (2004) Multi-objective calibration of land surface model evapotranspiration predictions using streamflow observations and spaceborne surface radiometric temperature retrievals. J Geophys Res 108(D23): 4725, doi:1029/2002JD003292

Diak GR, Whipple MS (1995) Estimating surface sensible heat fluxes using surface temperatures measured from a geostationary satellite during FIFE 1989 – Note. J Geophys Res 100(D12): 25453–25461

Gao H, Wood EF, Drusch M, McCabe MF (2007) Copula derived observation operators for assimilating TMI and AMSR-E soil moisture into land surface models. J Hydrometeorol 8(3): 413–429

Glenn EP, Huete AR, Nagler PL, Hirschboeck KK, Brown P (2007) Integrating remote sensing and ground methods to estimate evapotranspiration. Crit Rev Plant Sci 26(3):139–168

Gowda PH, Chavez JL, Colaizzi PD, Evett SR, Howell, TA, Tolk JA (2007) Remote sensing based energy balance algorithms for mapping ET: current status and future challenges. Trans Am Soc Agri Biol Eng (ASABE) 50(5):1639–1644

Jackson TJ, Cosh MH (2003a) SMEX02 watershed soil moisture data, Walnut Creek, Iowa. National Snow and Ice Data Center. Digital Media, Boulder, CO

Jackson TJ, Cosh MH (2003b) SMEX02 Landsat Thematic Mapper Imagery, Iowa. National Snow and Ice Data Center. Digital media, Boulder, CO

Kalma JD, McVicar TR, McCabe MF (2008) Estimating land surface evaporation: a review of methods using remotely sensed surface temperature data. Surv Geophys 29:421–469, doi: 10.1007/s10712-008-9037-z

King MD, Kaufman YJ, Menzel WP, Tanré D (1992) Remote sensing of cloud, aerosol, and water vapor properties from the Moderate Resolution Imaging Spectrometer (MODIS). IEEE Trans Geosci Remote Sens 30:2–27

Kumar SV, Peters-Lidard CD, Tian Y, Houser PR, Geiger J, Olden S, Lighty L, Eastman JL, Doty B, Dirmeyer P, Adams J, Mitchell K, Wood EF, Sheffield J (2006) Land Information System – An Interoperable Framework for High Resolution Land Surface Modeling. Environ Model Softw 21(10):1402–1415, doi:10.1016/j.envsoft.2005.07.004

Kustas WP, Norman JM (1996) Use of remote sensing for evapotranspiration monitoring over land surface. Hydrol Sci J 41(4):495–516

Kustas WP, Norman JM (1997) A two-source approach for estimating turbulent fluxes using multiple angle thermal infrared observations. Water Resour Res 33(6):1495–1508

Kustas WP, Li F, Jackson TJ, Prueger JH, MacPherson, JI, Wolde M (2004) Effects of remote sensing pixel resolution on modeled energy flux variability of croplands in Iowa. Remote Sens Environ 92(4):535–547

Kustas WP, Hatfield, JL, Prueger JH (2005) The Soil Moisture Atmosphere Coupling Experiment (SMACEX): background, hydrometeorological conditions and preliminary findings. J Hydrometeorol 6(6):791–804

Li, F, Kustas WP, Anderson MC, Prueger JH, Scott RL (2008) Effect of remote sensing spatial resolution on interpreting tower-based flux observations. Remote Sens Environ 112:337–349

Li F, Jackson TJ, Kustas WP, Schmugge TJ, French AN, Cosh, MH, Bindlish R (2004) Deriving land surface temperature from Landsat 5 and 7 during SMEX02/SMACEX. Remote Sens Environ 92(4):521–534

Liang S, Strahler AH, Walthall C (1999) Retrieval of land surface albedo from satellite observations: a simulation study. J Appl Meteorol 38(6):712–725

Luo L, Robock A, Mitchell KE, Houser PR, Wood EF, Schaake JC, Lohmann D, Cosgrove B, Wen F, Sheffield J, Duan Q, Higgins RW, Pinker RT, Tarpley JD (2003) Validation of the North American Land Data Assimilation System (NLDAS) retrospective forcing over the southern Great Plains. J Geophys Res 108:8843, doi:10.1029/2002JD003246

Margolis HA, Ryan MG (1997) A physiological basis for biosphere-atmosphere interactions in the boreal forest: an overview. Tree Physiol 17(8–9):491–499

McCabe MF, Kalma JD, Franks SW (2005) Spatial and temporal patterns of land surface fluxes from remotely sensed surface temperatures within an uncertainty modelling framework. Hydrol Earth Syst Sci 9(5):467–480

McCabe MF, Wood EF (2006) Scale influences on the remote estimation of evapotranspiration using multiple satellite sensors. Remote Sens Environ 105(4):271–285

McCabe MF, Balick LK, Theiler JP, Gillespie AR, Mushkin A (2008a) Forward modeling of linear mixing in thermal IR temperature retrieval. Int J Remote Sens 29: 5047–5061.

McCabe MF, Wood EF, Wójcik R, Pan M, Sheffield J, Su H, Gao H (2008b) Hydrological consistency using multi-sensor remote sensing data for water and energy cycle studies. Remote Sens Environ 112(2):430–444, doi:10.1016/j.rse.2007.03.027

McVicar TR, Jupp DLB (2002) Using covariates to spatially interpolate moisture availability in the Murray–Darling Basin: a novel use of remotely sensed data. Remote Sens Environ 79:199–212

Mitchell KE, Lohmann D, Houser PR, Wood EF, Schaake JC, Robock A, Cosgrove B, Sheffield J, Duan Q, Luo L, Higgins RW, Pinker RT, Tarpley JD, Lettenmaier DP, Marshall CH, Entin JK, Pan M, Shi W, Koren V, Meng J, Ramsay BH, Bailey AA (2004) The multi-institution North American Land Data Assimilation System (NLDAS): utilizing multiple GCIP products and partners in a continental distributed hydrological modeling system. J Geophys Res 109(D7): doi:10.1029/2003JD003823

Norman JM, Anderson MC, Kustas WP, French AN, Mecikalski JR, Torn RD, Diak GR, Schmugge, TJ, Tanner BCW (2003) Remote sensing of surface energy fluxes at 10^1-m resolutions. Water Resour Res 39(8):1221, doi:10.1029/2002WR001775

Norman JM, Kustas WP, Prueger, JH, Diak GR (2000) Surface flux estimation using radiometric temperature: a dual temperature-difference method to minimize measurement errors. Water Resour Res 36(8):263–2274

Nunez M, Kalma JD (1996) Satellite mapping of the surface radiation budget. In: Stanhill G (ed) Advances in bioclimatology. Springer-Verlag, Berlin, pp 63–124

Pan M, Wood EF, Wójcik R, McCabe MF (2008) Estimation of the regional terrestrial water cycle using multi-sensor remote sensing observations and data assimilation. Remote Sens Environ 112(4):1282–1294, doi:10.1016/j.rse.2007.02.039

Pinker RT, Laszlo I (1992) Modelling surface solar irradiance for satellite applications on a global scale. J Appl Meteorol 31:194–211

Pinker RT, Wang H, King MD, Platnick S (2003) The first use of MODIS data to cross-calibrate with GEWEX/SRB datasets. GEWEX News 13(4)

Prata AJ, Caselles V, Coll C, Sobrino JA, Ottle C (1995) Thermal remote sensing of land surface temperature from satellites: current status and future prospects. Remote Sens Rev 12:175–224

Prueger JH, Hatfield JL, Kustas WP, Hipps LE, Li F, Macpherson I, Anderson MC, Parkin TB, Eichinger WE, Cooper DJ (2005a) Spatial and temporal variation of water, energy and carbon fluxes from tower and aircraft measurements. American Meteorological Society Conference Paper, 5 p.

Prueger JH, Hatfield JL, Kustas WP, Hipps LE, MacPherson JI, Neale CMU, Eichinger WE, Cooper DI, Parkin TB (2005b) Tower and aircraft eddy covariance measurements of water vapor, energy, and carbon dioxide fluxes during SMACEX. J Hydrometeorol 6(6):954–960

Quattrochi DA, Luvall FJC (1999) Thermal infrared remote sensing for analysis of landscape ecological processes: methods and applications. Landscape Ecol 14:577–598

Raupach MR, Finnigan JJ (1995) Scale issues in boundary-layer meteorology: surface energy balance in heterogeneous terrain. Hydrol Processes 9:589–612

Rodell M, Houser PR, Jambor U, Gottschalck J, Mitchell K, Meng J, Arsenault K, Cosgrove B, Radakovich J, Bosilovich M, Entin JK, Walker JP, Lohmann D, Toll D (2004) The global land data assimilation system. Bull Am Meteorological Soc 85(3):381–394

Rogers E, Black TL, Deaven DG, Dimego GJ, Zhao Q, Baldwin M, Junker NW, Lin Y (1996) Changes to the operational "Early" Eta analysis/forecast system at the National Centers for Environmental Prediction. Weather Forecasting 11:391–413

Schaaf CB, Gao F, Strahler AH, Lucht W, Li X, Tsang T, Strugnell NC, Zhang X, Jin Y, Muller J-P, Lewis P, Barnsley M, Hobson P, Disney M, Roberts G, Dunderdale M, Doll C, d'Entremont R, Hu B, Liang S, Privette JL (2002) First operational BRDF, albedo and nadir reflectance products from MODIS. Remote Sens Environ 83:135–148

Su Z (2000) Remote sensing of land use and vegetation for mesoscale hydrological studies. Int J Remote Sens 21:213–233

Su Z (2002) The surface energy balance system (SEBS) for the estimation of turbulent heat fluxes. Hydrol Earth Syst Sci 6(1):85–99

Su H, McCabe MF, Wood EF, Su Z, Prueger JH (2005) Modeling evapotranspiration during SMACEX02: comparing two approaches for local and regional scale prediction. J Hydrometeorol 6(6):910–922

Su H, Wood EF, McCabe MF, Su Z (2007) Evaluation of remotely sensed evapotranspiration over the CEOP EOP-1 reference sites. J Meteorol Soc Jpn 85A:439–459

Su H, Wood EF, Wang H, Pinker RT (2008) Spatial and temporal scaling behavior of surface shortwave downward radiation based on MODIS and in-situ measurements. Geophys Res Lett 5(3):542–546, doi: 10.1109/LGRS.2008.923209.

Trenberth KE (1999) Atmospheric moisture recycling: role of advection and local evaporation. J Climate 12:1368–1381

Twine TE, Kustas WP, Norman JM, Cook DR, Houser PR, Meyers TP, Prueger JH, Starks PJ, Wesely ML (2000) Correcting eddy-covariance flux underestimates over a grassland. Agric For Meteorol 103(3):279–300

Verstraeten WW, Veroustraete F, Feyen J (2008) Assessment of evapotranspiration and soil moisture content across different scales of observation. Sensors 8:70–117

Wan Z, Zhang Y, Zhang Q, Li Z-L (2002) Validation of the land-surface temperature products retrieved from Terra Moderate Resolution Imaging Spectroradiometer data. Remote Sens Environ 83:163–180

Wang Z, Heng X, Barlage M, Dickinson RE, Gao F, Schaaf CB (2004) Using MODIS BRDF and albedo data to evaluate global model land surface albedo. J Hydrometeorol 5(1):3–14

Xavier AC, Vettorazzi CA (2004) Mapping leaf area index through spectral vegetation indices in a subtropical watershed. Int J Remote Sens 25(9):1661–1672